Supporting Information

Structural domain plasticity drives Zn(II) distribution and buffering in metallothionein-3

Manuel David Peris-Díaz[1,2], Eduard H. T. M. Ebberink[1], Jan Fiala[1,§], Albert J. R. Heck[1], Artur Krężel[2*]

1 Biomolecular Mass Spectrometry and Proteomics, Bijvoet Center for Biomolecular Research and Utrecht Institute for Pharmaceutical Sciences, Utrecht University, Utrecht 3584 CH, The Netherlands

2 Department of Chemical Biology, Faculty of Biotechnology, University of Wrocław, F. Joliot–Curie 14a, 50–383 Wrocław, Poland

TABLE OF CONTENTS

Materials. 2
Expression and purification of metallothionein-3 2
Ion mobility-mass spectrometry 3
High resolution native MS and top-down HCD MS. 4
Native top-down ultraviolet photodissociation (UVPD) experiments....4
Single and double Cys labeling. 4
Steered molecular dynamics (SMD) simulations.. 5
Figure S1....6
Figure S2....7
Figure S3....8
Figure S4....9
Figure S5....10
Figure S6....11
Figure S7....12
Figure S8....12
Figure S9....13
REFERENCES 14

EXPERIMENTAL SECTION

Materials. The reagents used in this study were purchased from Sigma-Aldrich, Merck, Acros Organics, Roth, BioShop, VWR International (Avantor), and Iris-Biotech GmbH. The following reagents: $ZnSO_4 \cdot 7H_2O$, 4-(2-pyridylazo)resorcinol (PAR), $(NH_4)_2CO_3$, tris(hydroxymethyl)aminomethane (Tris base) and 4-(2-hydroxyethyl)-1 piperazineethanesulfonic acid (HEPES), mass spectrometry grade methanol, tris(2carboxyethyl)phosphine hydrochloride (TCEP), ammonium acetate (AmAc), ammonium bicarbonate, ethylenediamine-tetraacetic acid (EDTA), and mass spectrometry grade acetonitrile (ACN) were purchased from Sigma-Aldrich. Resin Chelex 100 was acquired from Bio-Rad and 98% hydrochloric acid (HCl) was purchased from VWR Chemicals. DL-dithiothreitol (DTT) was purchased from Iris Biotech GmbH. Tryptone, LB broth, yeast extract, isopropyl-β-D-1-thiogalactopyranoside (IPTG), and SDS were from Lab Empire, NaCl, NaOH, glycerol, $KH_2PO_4 \cdot H_2O$, K_2HPO_4 from POCH (Gliwice Poland), pTYB21 vector and chitin resin were from New England BioLabs, and 5,5′-dithiobis-(2-nitrobenzoic acid) (DTNB) from TCI Europe.

Expression and purification of metallothionein-3. The expression vector (Addgene plasmid ID 105710) containing metallothionein was transformed into BL21(DE3) *E. coli* cells, which were then grown in a culture medium (1.1% tryptone, 2.2% yeast extract, 0.45% glycerol, 1.3% K_2HPO_4, 0.38% KH_2PO_4) at 37°C until ~0.8 OD_{600}. Protein expression was induced by adding 0.1 mM IPTG along with 0.5 M $ZnSO_4$ to the cells, followed by overnight incubation at 20°C with shaking. Subsequent steps were performed at 4°C. The cells were harvested by centrifugation at 4,000 · *g* for 10 min and then resuspended in 50 ml of cold buffer A (20 mM HEPES, pH 8.0, 500 mM NaCl, 1 mM EDTA, 1 mM TCEP). After sonication for 45 min (using 5 s sonication and 10 s pause cycles), the cell lysate was obtained by centrifugation at 16,000 · *g* for 15 min. The resulting supernatant was loaded onto a chitin resin and incubated overnight with buffer A (20 ml). Following this, the resin was washed with buffer A (50 ml) and treated with 100 mM DTT for cleavage. The resin was then incubated on a rocking bed at room temperature for 48 h. The eluted solution from the chitin column was concentrated using Amicon Ultra-4 Centrifugal Filter Units with a 3 kDa membrane cut-off (Merck Millipore, USA). Subsequently, the pH of the concentrated solution was lowered to approximately 2.5 by adding 7% HCl, and another centrifugation step was performed. The protein was then purified

on a size exclusion chromatography using a HiLoad 16/600 Superdex 75 pg gel filtration column (Cytiva, USA) equilibrated with 10 mM HCl at 1 ml/min flow rate using an ÄKTA Pure system.[1] The identity of the protein in the eluted fractions was confirmed using ESI-MS with a Bruker Maxis Impact (Bruker Daltonik GmbH, Bremen, Germany) calibrated with a commercial ESI-TOF Tuning mix (Sigma-Aldrich). The concentration of thiols was determined spectrophotometrically using a DTNB assay[2], while the Zn(II) binding capacity was confirmed spectrophotometrically by Zn(II) and Cd(II) titrations.[3] After obtaining the purified apoMT3, an 8.5 molar excess of $ZnSO_4$ was added to it in the presence of a nitrogen blanket, and 1 mM TCEP to prevent oxidation. The pH of the solution was adjusted to 8.6 using a 1 M Tris base. The resulting mixture was concentrated using Amicon Ultra-4 Centrifugal Filter Units with a 3 kDa membrane cut-off (Merck Millipore, USA). Subsequently, the concentration samples were subjected to purification on a SEC HiLoad 16/600 Superdex 75 pg gel filtration column (Cytiva, USA) that had been equilibrated with 20 mM Tris-HCl buffer at pH 8.6. The concentrations of thiols and Zn(II) were determined spectrophotometrically using DTNB and PAR assays, respectively.[4]

Ion mobility-mass spectrometry. IM-MS experiments were carried out on a Synapt XS HDMS instrument equipped with nanoelectrospray ionization (Waters Corporation, Manchester, UK). The ion source was operated under gentle conditions to prevent ion activation (source temperature 30 °C, cone voltage 10 V, source offset 1). Experiments were carried out in sensitivity mode. 5–10 μL of (10 μM in 200 mM ammonium acetate) was loaded into borosilicate glass capillaries (O.D. 1.2 mm, I.D. 0.9 mm, World Precision Instruments, Stevenage, UK) produced in-house using a Flaming/Brown P-1000 micropipette puller (Sutter Instrument Co., Novato, CA, USA), and ions were produced by applying a positive potential of 0.9–1.4 kV via a platinum wire (Goodfellow). Traveling wave (TW) velocity and height used were 300 ms^{-1} and 20 V, respectively. Collision-induced unfolding (CIU) experiments were performed by increasing the trap collision energy (0–60 V) of quadrupole-selected ions and recording ion arrival time distributions. Measurements were performed in triplicate on different days to account for potential sources of variation, and the data were averaged. Ubiquitin (bovine), cytochrome C (equine heart), and β-lactoglobulin (bovine milk) purchased from Sigma-Aldrich were dissolved in 200 AmAc, diluted to 10 μM, and used to calibrate the TW device. The literature CCS_{N2} values for the standards were obtained from A. P. France et al.[5]. CCS calibration was performed using IMSCal19 (Waters Corp., UK) [6]. Data were analyzed by means of Masslynx v4.2 (Waters Corp., UK) and custom Python 3.5 scripts.

High resolution native MS and top-down HCD MS. Chemical labeling mass spectrometry (MS) and top-down MS experiments were performed on a Thermo Scientific Orbitrap Fusion mass spectrometer (Thermo Fisher Scientific, Bremen, Germany) equipped with nESI source. Samples were electrosprayed using gold-coated borosilicate capillaries pulled in-house. All data were acquired in the Orbitrap mass analyzer at a resolution of 240,000. Sixty scans, each with 1 microscan were averaged. Data was acquired using a mass range of 200-300 m/z. For top-down HCD, precursor ion isolation was performed with a quadrupole analyzer, and the isolation window was set to 25 m/z. The precursor automatic gain control (AGC) target value was 5e5, maximum injection time 150 ms, and a normalized collision energy (NCE) was set to 15-50%. Optimal fragmentation was found using NCE 27% (70.3 V) and in-source CID 20V. Data was processed using Xcalibur 4.1 and Python 3.5 scripts. For EThcD, a 5-30 ms reaction time and 5-15% supplemental HCD were used.

Native top-down ultraviolet photodissociation (UVPD) experiments. Experiments were performed on a previously described extended mass range (EMR) Q-Exactive Orbitrap (Thermo Fisher Scientific, Bremen, Germany) modified to enable UVPD[7]. Briefly, the charge detector was removed from the HCD-cell to introduce a laser beam into the HCD cell. The UVPD spectra were acquired using 6 ns laser pulses at a wavelength of 193 nm and an energy of 6 mJ $pulse^{-1}$ (ExciStar 500 UV laser, Coherent, Santa Clara, CA). Data were collected with the noise threshold parameter set to 3.64, fixed injection time to 250 ms, and a FT resolution of 140000. The ion transfer optics (injection flatapole, interflatapole lens, bent flatapole) were set to 9, 7, and 5 V, respectively. Around 100 scans with 1 microscan each were collected and subsequently averaged. Data was processed using Xcalibur 4.1, mMass[8] and Python 3.5 scripts.

Single and double Cys labeling. The Zn_7MT3_{red} stock (0.640 mM) was diluted to 30 μM in 200 mM ammonium acetate (pH 6.8), and various amounts of iodoacetamide (25, 50, 75, 125, or 150 mM) were added to reach a final protein concentration of 15 μM. The mixtures were then incubated in the dark at 25°C for 15 min. The samples were then desalted using 7 kDa cut-off Zeba spin desalting columns (Thermo Fisher Scientific, USA) equilibrated with 200 mM ammonium acetate (pH 6.8). IAM-labeled samples were diluted to 2 μM for native MS or top-down CID. For double labeling, proteins were incubated with 50 mM NEM at 25°C for 30 min. Samples were then desalted and diluted prior to MS analysis.

Steered molecular dynamics (SMD) simulations. The initial Zn_7MT3 coordinates were obtained using AlphaFold[9]. The protonation states of the side chains at pH 7.0 were assigned using PROPKA, except for the Cys residues that were deprotonated. The AMBER FF19SB force field and recently published cysteine-Zn(II) force field parameters were used to model the protein and the Cys residues[10]. Zn_7MT3 was solvated in an 8 Å cubic box using TIP3P water molecules, and NaCl replaced water molecules to achieve neutrality. The system was then energy-minimized using steepest descent and equilibrated in the NVT ensemble using the Langevin thermostat (0 to 300 K with a damping coefficient of 1 ps^{-1}). Then, the system was equilibrated in the NPT ensemble at a constant pressure (1 atm) and temperature (300 K) for 100 ns using Berendsen weak coupling. Then, 100 ns were run using the Parinello-Rahman barostat and the Nosé-Hoover thermostat. To evaluate electrostatic interactions, the particle mesh Ewald (PME) algorithm was used, using a cut-off of 8 Å. The LINCS algorithm was used to constrain bonds only involving hydrogen atoms to allow the use of a 2 fs time step.

SMD simulations were performed by coupling GROMACS 2018.4 with the PLUMED 2.6 plugin[11-12]. Initially, we run 10 independent SMD simulations for each Zn(II) site in Zn_7MT3, for a total of 70 runs. For each Zn(II) site, we defined a collective variable (CV) that measures the distance between the Zn(II) ion and the center of mass of the initially four Cys residues to which it is bound. To evaluate the energy required to dissociate Zn(II) from the protein, we applied a 10 kcal·mol^{-1} positional restraint to all CA protein backbone atoms. We used a force constant of 100 kcal·mol^{-1} and pulling speed of 100 Å·ns^{-1}, as we determined a good choice for this type of simulations [13]. We calculate the contact number (CN) between Zn(II) and each sulfur ligand as defined as:

$$CN_{Zn-S} = \sum_{i \in A} \sum_{i \in B} s_{ij} \qquad (1)$$

where A is the Zn(II) ion, B corresponds to the Cys(S) residue, and s_{ij} is a switching function. The switching function is defined as:

$$s_{ij} = \frac{1 - \left(\frac{r_{ij}}{r_0}\right)^n}{1 - \left(\frac{r_{ij} -}{r_0}\right)^m} \qquad (2)$$

Where n = 8 and m =12, and they define the steepness of the switching function, and r_o = 2.8 Å, which defines the cut-off to where the interactions between Zn(II) and S are calculated. We

carried out 10 SMD trajectories for each of the seven Zn(II) sites in Zn_7MT3 and defined the weakest site as the one requiring the lowest dissociation work. The final frame of a trajectory pulling from this site was used to seed the Zn_6MT3 model. The Zn_5MT3 model was subsequently generated using the same workflow.

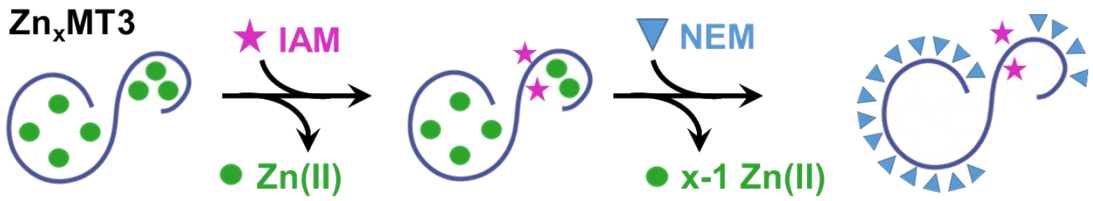

Figure S1. Schematic overview of the differential labeling strategy used for mapping Zn(II) binding sites. In the first step, Zn(II) is displaced stepwise from Zn7MT3 as increasing amounts of IAM are added. In the second step, the remaining bound Zn(II) is removed by treatment with excess NEM.

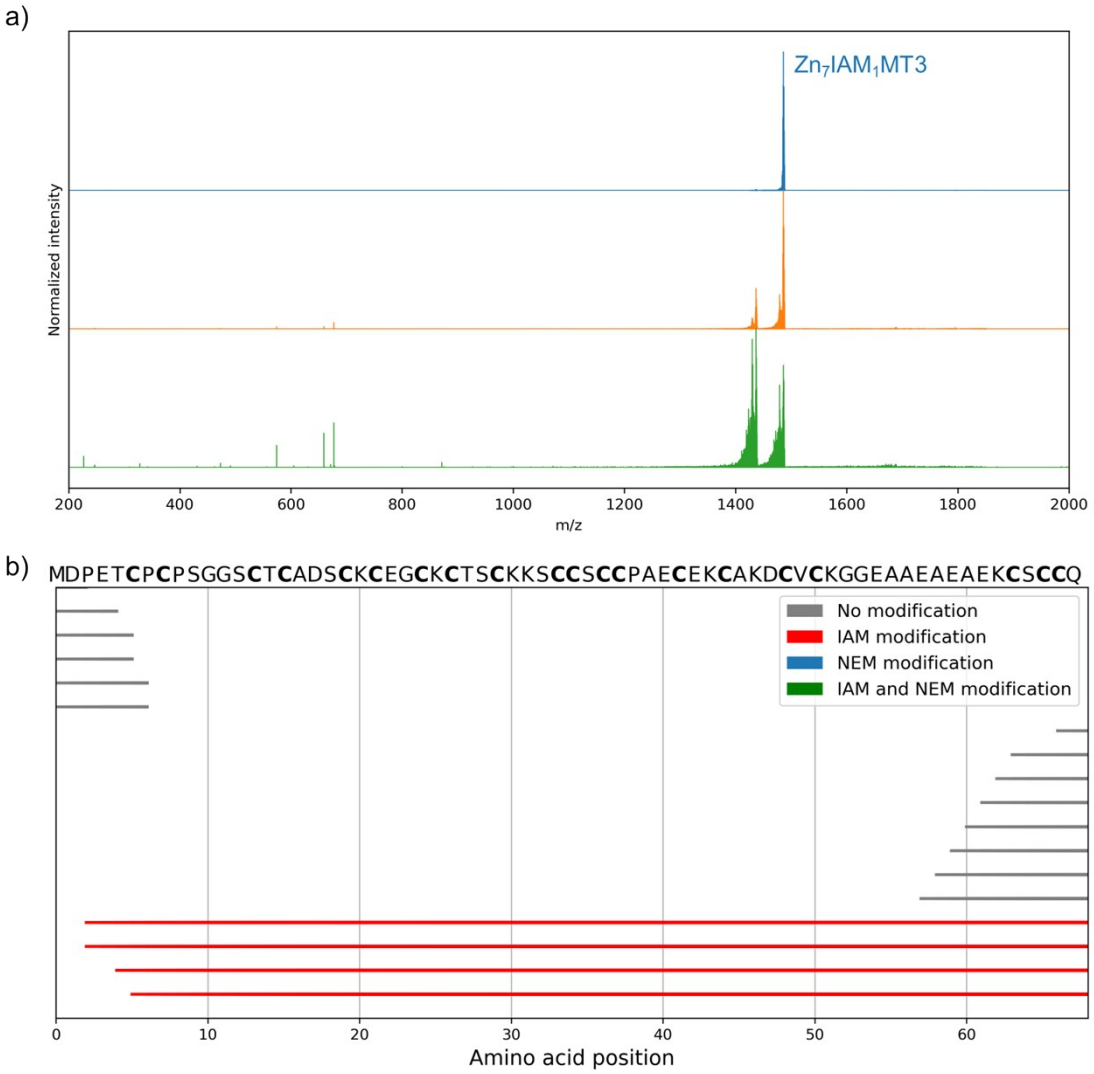

Figure S2. Top-down CID MS of quadrupole-isolated $Zn_7IAM_1MT3^{5+}$ ions at different HCD energies (a). Fragmentation map for isolated 1485 *m/z* ions and fragmented using HCD NCE 27%.

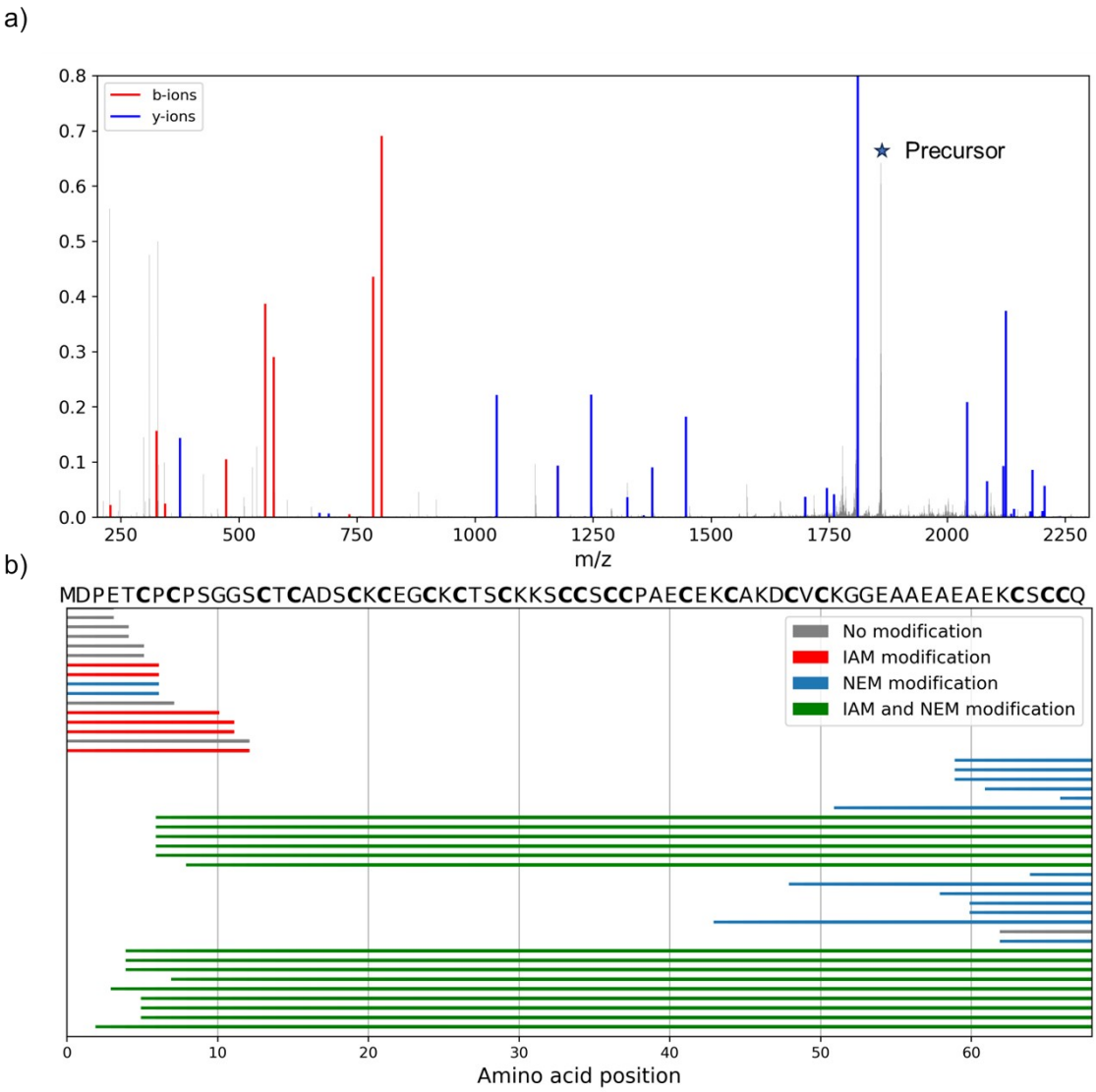

Figure S3. Top-down CID MS of quadrupole-isolated $NEM_{19}IAM_2MT3^{5+}$ ions at HCD NCE 27% (a) and its fragmentation map (b).

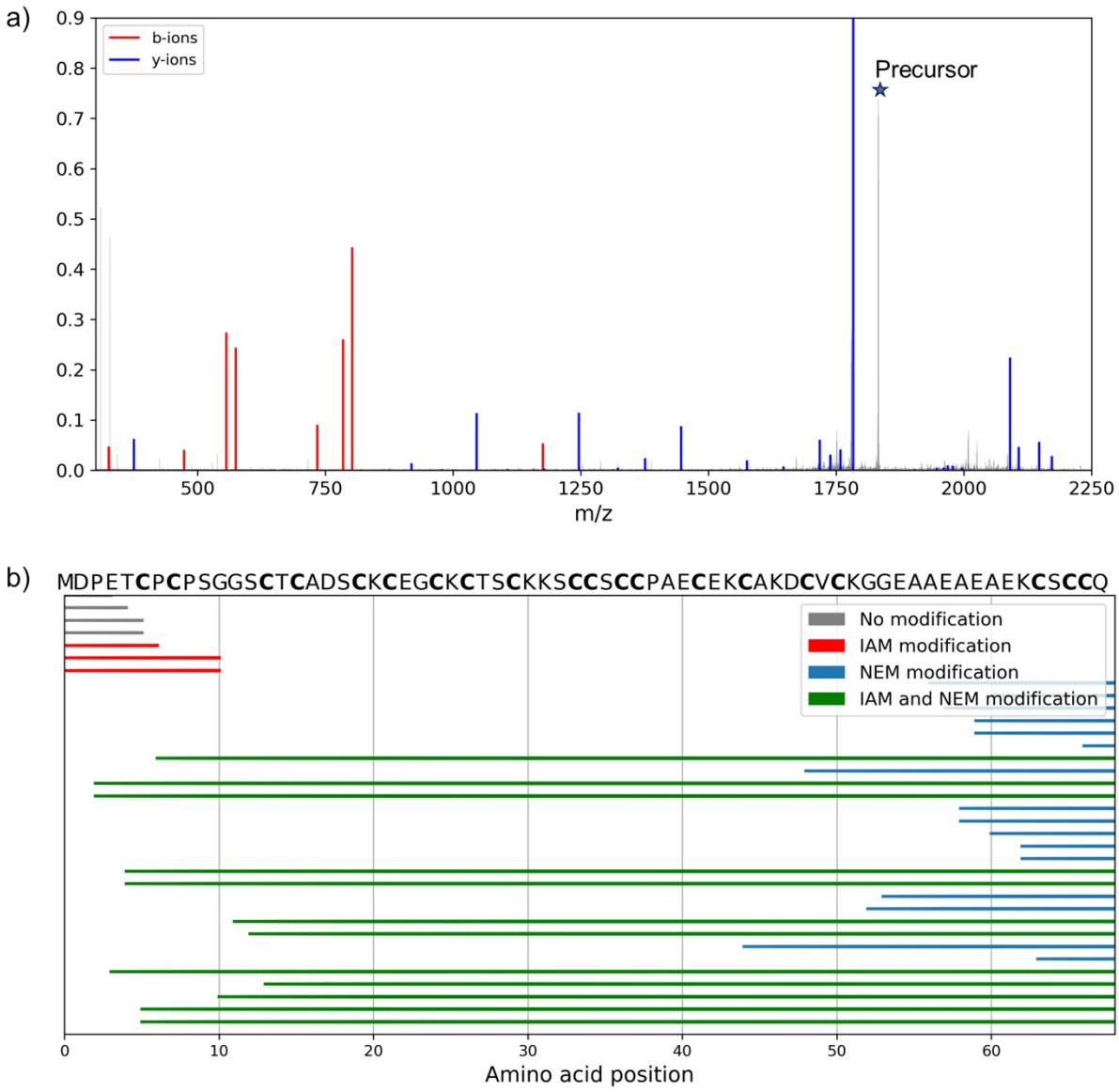

Figure S4. Top-down CID MS of quadrupole-isolated $NEM_{16}IAM_4MT3^{5+}$ ions at HCD NCE 27% (a) and its fragmentation map (b).

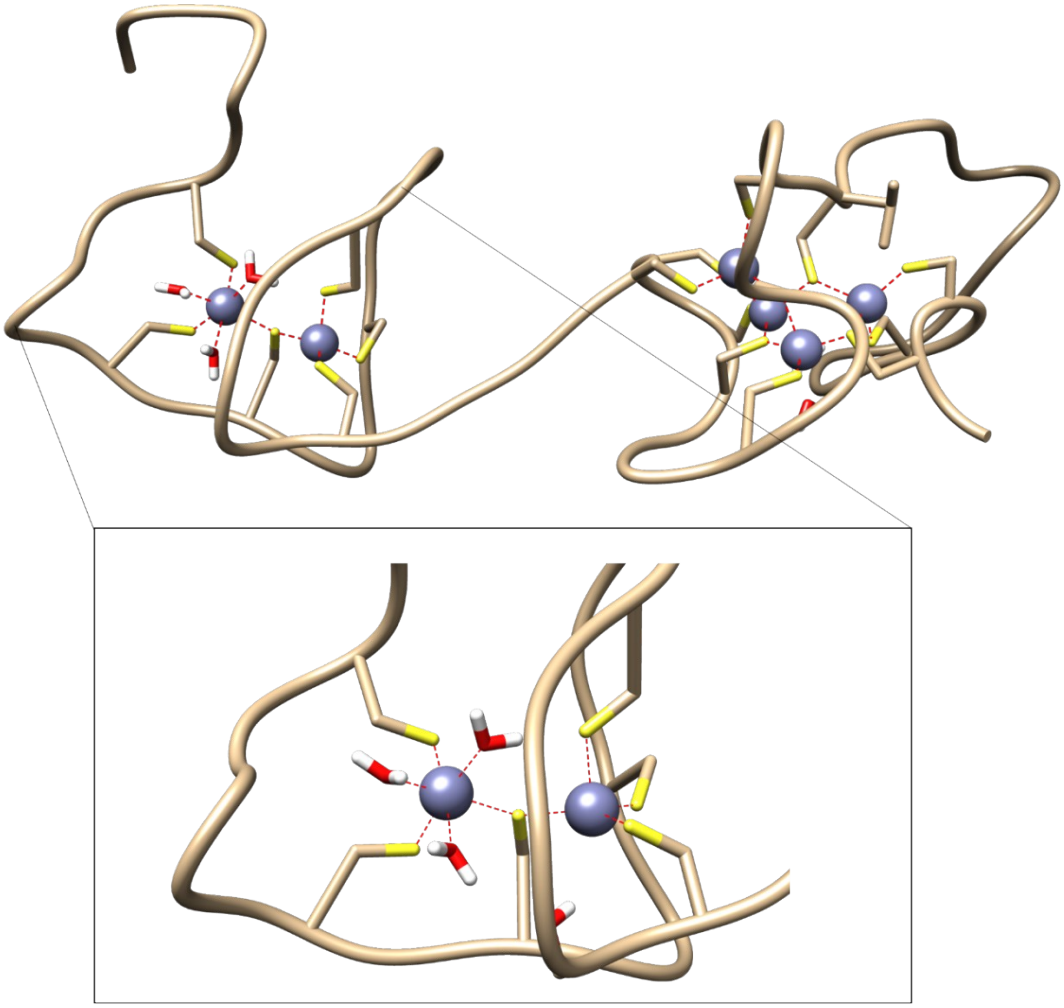

Figure S5. Representative frame of Zn_6MT3 from steered molecular dynamics (SMD) simulations. Zoom in for the Zn_2Cys_6 cluster in the β–domain. As a result of Zn(II) dissociation, one Zn(II) ion is coordinated by three cysteine residues, with the remaining coordination sites occupied by solvent molecules, consistent with a labile coordination enviroment. This results in a distorded octahedral geometry.

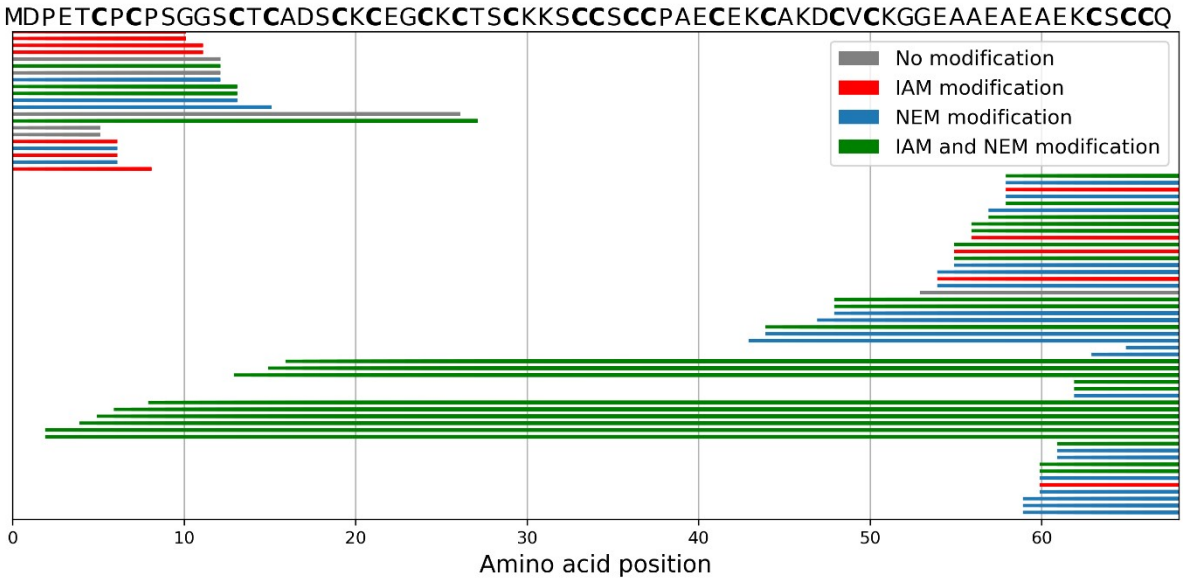

Figure S6. Fragmentation map from top-down CID MS of quadrupole-isolated $NEM_{14}IAM_6MT3^{5+}$ ions acquired at HCD NCE 27%.

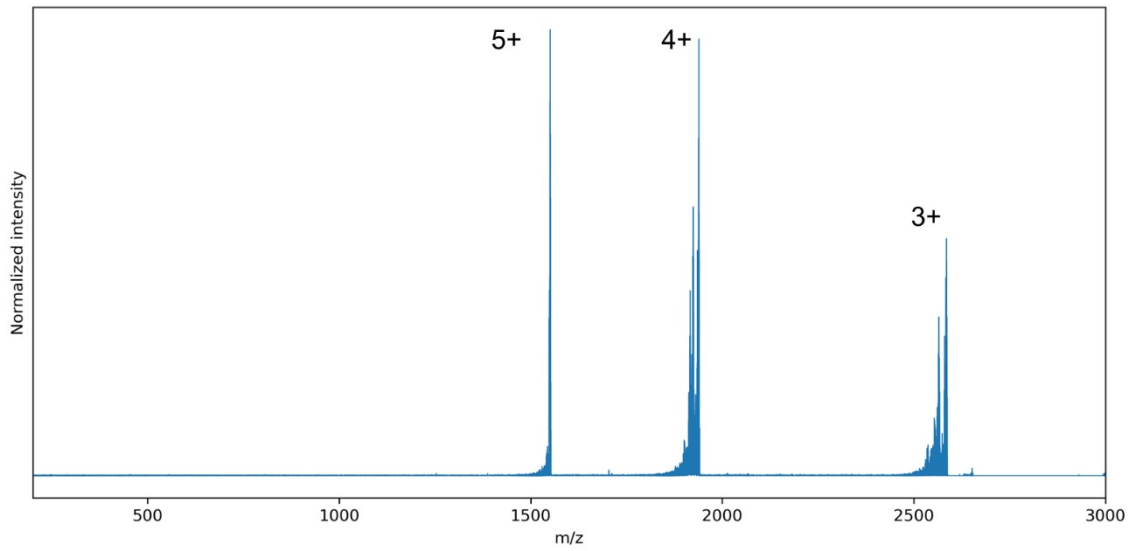

Figure S7. Top-down electron-transfer/higher-energy collision dissociation (EThcD) MS for quadrupole-selected $Zn_4IAM_{10}MT3^{5+}$ ions.

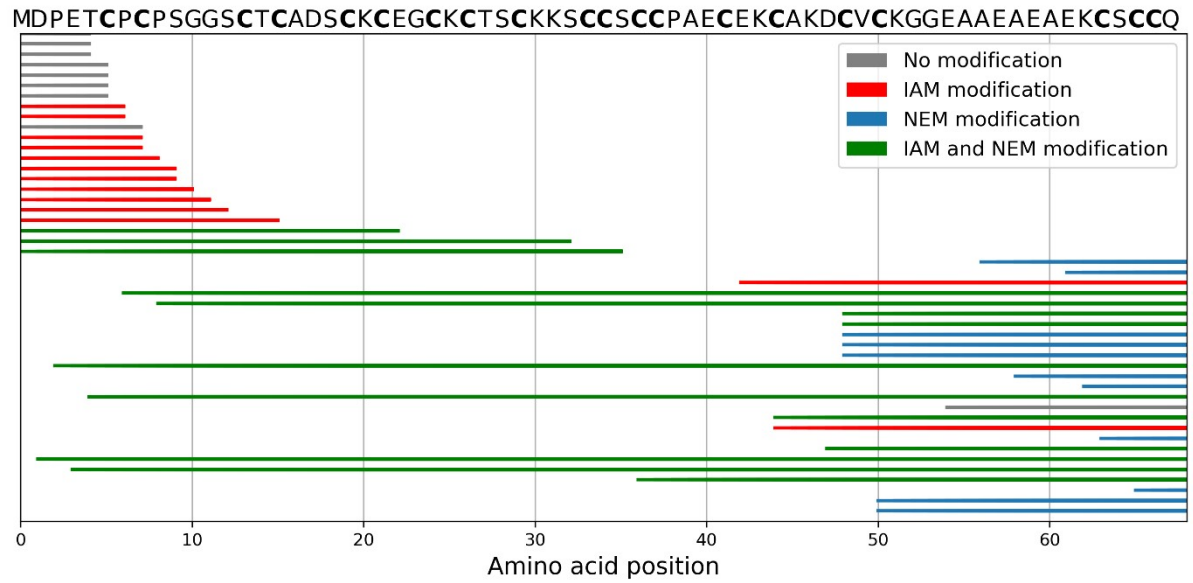

Figure S8. Fragmentation map from top-down ultraviolet photodissociation (UVPD) MS of quadrupole-isolated $NEM_{10}IAM_{10}MT3^{5+}$ ions.

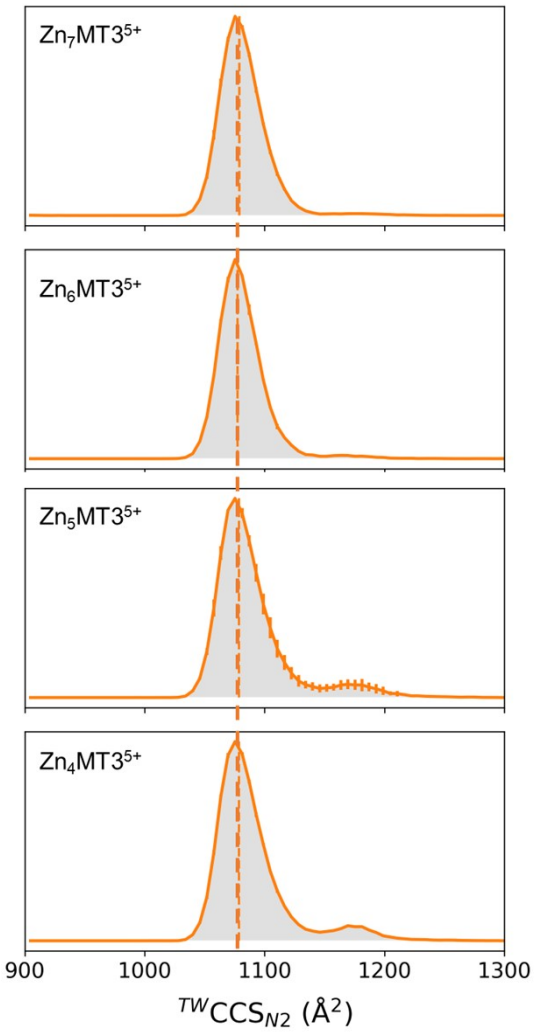

Figure S9. Native travelling–wave ion mobility MS (TWIM-MS)–derived collision cross-section profiles of $Zn_{7\text{-}4}MT3^{5+}$ ions.

REFERENCES

1 Krężel, A.; Maret, W. The bioinorganic chemistry of mammalian metallothioneins. *Chem. Rev.* **2021**, *121*, 14594–14648.

2 Eyer, P.; Worek, F.; Kiderlen, D.; Sinko, G.; Stuglin, A.; Simeon-Rudolf, V.; Reiner, E. Molar absorption coefficients for the reduced Ellman reagent: reassessment. *Anal. Biochem.* **2003**, *312*, 224–227.

3 Peris-Díaz, M. D.; Guran, R.; Domene, C.; de los Rios, V.; Zitka, O.; Adam, V.; Krężel, A. An integrated mass spectrometry and molecular dynamics simulations approach reveals the spatial organization impact of metal-binding sites on the stability of metal-depleted metallothionein-2 species. *J. Am. Chem. Soc.* **2021**, *143*, 16486–16501.

4 Peris-Díaz, M. D.; Guran, R..; Zitka, O.; Adam, V.; Krężel, A. Metal- and affinity-specific dual labeling of cysteine-rich proteins for identification of metal-binding sites. *Anal. Chem.* **2020**, *92*, 12950–12958.

5 France, A. P.; Migas, L. G.; Sinclair, E.; Bellina, B.; Barran, P. E. Using collision cross section distributions to assess the distribution of collision cross section values. *Anal. Chem.* **2020**, *92*, 4340–4348.

6 Richardson, K.; Langridge, D.; Dixit, S. M.; Ruotolo, B. T. An improved calibration approach for traveling wave ion mobility spectrometry: robust, high-precision collision cross sections. *Anal. Chem*. **2021**, *93*, 3542–3550.

7 Fort, K.L; Dyachenko, A.; Potel, C. M.; Corradini, E.; Marino, F.; Barendregt, A.; Makarov, A. A.; Scheltema, R. A.; Heck, A. J. R. Implementation of ultraviolet photodissociation on a benchtop Q Exactive mass spectrometer and its application to phosphoproteomics. *Anal. Chem*. **2016**, *88*, 2303–2310.

8 Strohalm, M.; Kavan, D.; Novák, P.; Volný, M.; Havlíček, V. mMass 3: a cross-platform software environment for precise analysis of mass spectrometric data. *Anal. Chem*. **2010**, *82*, 4648–4651.

9 Jumper, J. et al. Highly accurate protein prediction with AlphaFold. *Nature*, **2021**, *596*, 583–589.

10 Macchiagodena, M.; Pagliai, M.; Andreini, C.; Rosato, A.; Procacci, P. Upgrading and validation of the AMBER force field for histidine and cysteine zinc(II)-binding residues in sites with four protein ligands. *J. Chem. Inf. Model.* **2019**, *59*, 3803–3816.

11 Van Der Spoel, D.; Lindahl, E.; Hess, B.; Groenhof, G.; Mark, A. E.; Berendsen, H. J. GROMACS: Fast, flexible, and free. *J. Comput. Chem*. **2005**, *26*, 1701–1718.

12 PLUMED Consortium. Promoting transparency and reproducibility in enhanced molecular simulations. *Nat. Methods* **2019**, *16*, 670–673.

13 Singh, A. K.; Pomorski, A.; Wu, S.; Peris-Diaz, M. D.; Czepczyńska-Krężel, H.; Krężel, A. The connection of α- and β-domains in mammalian metallothionein-2 differentiates Zn(II) binding affinities, affects folding, and determines zinc buffering properties. *Metallomics*, **2023**, *15*, mfad029.